

The study of RDX impurity and wax effects on the thermal decomposition kinetics of HMX explosive using DSC/TG and accelerated aging methods

H. Sinapour¹ · S. Damiri¹ · H. R. Pouretedal¹

Received: 9 October 2016 / Accepted: 22 January 2017 / Published online: 9 February 2017
© Akadémiai Kiadó, Budapest, Hungary 2017

Abstract The thermal decomposition kinetic behavior of three HMX explosive samples containing 5.0 mass% (A-HMX) and 0.5 mass% RDX impurity (B-HMX) and HMX desensitized with 5.0 mass% paraffin wax (W-HMX) was studied by non-isothermal differential scanning calorimetric and thermogravimetric techniques at different temperature scan rates and by isothermal accelerated aging method. Using KAS isoconversional method, the mean activation energies of 229.36, 221.05, and 267.37 kJ mol⁻¹ were obtained for B-HMX, A-HMX, and W-HMX, respectively, showing the higher thermal stability of pure and desensitized HMX. Moreover, the reaction mechanism was found in Avrami–Erofeev A2 model for all samples. In this study, by using the calculated kinetics triplets, the chemical lifetime of explosives were predicted based on 5.0 mass% mass loss and were compared with isothermal accelerated aging results, under two constant temperatures. The experimental results in the higher temperatures demonstrated relatively better consistency with predicted values.

Keywords HMX explosive · RDX and wax · DSC/TG · Kinetic triplet · Activation energy

Introduction

Octahydro-1,3,5,7-tetranitro-1,3,5,7-tetrazocine, or High Melting eXplosive (HMX), is one of the highly energetic material widely used for various applications like high explosive compositions for mass destructive warheads, as an energetic additive in the most advanced gun and rocket solid propellants and also perforation in oil well industries [1, 2]. HMX, also known as Octogen, is a powerful and relatively insensitive polynitramine high explosive, chemically related to its similar nitramine explosive homolog of 1,3,5-trinitro-1,3,5-triazacyclohexane (RDX). One of the common methods of manufacturing HMX is nitration of hexamine in the presence of acetic anhydride, paraformaldehyde, and ammonium nitrate. The crude HMX produced in this process usually contains 10–20 mass% RDX as an impurity [3]. In line with the US military standard for HMX [4], this explosive is produced and used as two types of A, with maximum RDX content of 7.0 mass%, and B, with maximum RDX content of 2.0 mass%. Recently, it has been specified that other HMX grades, like reduced sensitivity HMX or insensitive HMX, containing the least amount of HMX impurity, show low sensitivity to explosive shocks in melt-casting and plastic-bonded explosives. One of the main reasons for the above behavior is to the presence of RDX impurity in HMX, which can lead to the generation of many defects in the crystal lattice of HMX [5–7]. Also to desensitize the pure HMX explosive, various desensitizing agents like polymers and waxes were added to produce various standard explosive and propellant formulations [8, 9]. Desensitized waxes are one of the most effective compounds for absorbing and desensitizing the initiation of explosive materials by impact, friction, or static electricity stimuli [9–12].

In different countries around the world, due to explosive storage or transportation, many unexpected runaway

✉ S. Damiri
s_damiri@mut-es.ac.ir

¹ Department of Applied Chemistry, Maleke-ashtar University of Technology, Shahin-shahr, Esfahan, Iran

accidents can occur [13]. Because of the explosive nature of these materials, study on aging and kinetic parameters like the activation energy (E_a), the pre-exponential factor (A) and the reaction model are necessary. These parameters are closely dependent on purity and/or some additives, and they provide various useful information about safety, thermal stability, and chemical lifetime parameters [14–17]. In recent years, there are some approaches to accelerated aging methods which play an essential role in assessing the lifetime of manufactured products. Aging evaluation under ambient temperature takes long time. Therefore, the accelerated aging method is employed [16, 17].

Thermal analysis methods such as differential scanning calorimeter (DSC) and thermogravimetry (TG) due to high sensitivity can provide detailed information on the mechanism of ignition reactions, thermokinetics parameters, and lifetime studies [15, 18–20]. Among several methods for the analysis of DSC data, the isoconversional method has been recommended as a trustworthy method for determining reliable and consistent activation energies of solid-state reactions [21]. In fact, the isoconversional methods can determine the actual value of E_a from DSC data without the knowledge of the kinetic model [22–25]. Vyazovkin et al. [26] in Kinetics Committee of the International Confederation for Thermal Analysis and Calorimetry (ICTAC) presented some recommendations to improve the accurate methodology for determining kinetic parameters. These recommendations were applied for reliable estimation of kinetic parameters such as activation energy and pre-exponential factor, and determination of the reaction model for thermal ignition of explosive composition. Here, the activation energy for the ignition process can be calculated using KAS (Kissinger, Akahira, Sunose) method based on DSC data at different heating rates. In addition, the compensation effect method can be used for accurate determination of the reaction model and pre-exponential factor.

Up to now, some researches have reported about thermal decomposition of HMX [27–29] and HMX-based explosive formulations, including the effect of some contaminants such as the catalytic effect of some metals nanometal powders [30], $\text{FeCl}_2 \cdot 4\text{H}_2\text{O}$, $\text{FeCl}_3 \cdot 6\text{H}_2\text{O}$, acetone, acetic acid, nitric acid [13], KClO_3 [31], plastic-bonded explosives [32], and C4 explosive matrix [33]. There are a wide range of activation energies and pre-exponential factors for HMX based on type of method and different mathematical estimations [27, 34].

In this study, the influence of RDX impurity and paraffin wax additive on kinetic triplet (E_a , pre-exponential factor and reaction model) and aging behavior of HMX grade A with RDX content of 5.0 mass% (A-HMX), HMX grade B with RDX content of 0.5 mass% (A-HMX), and B-HMX

desensitized by 5.0 mass% paraffin wax (W-HMX) were examined and compared by non-isothermal thermogravimetry (TG) and differential scanning calorimetry (DSC). In addition, mass loss of the mentioned samples were predicted and compared to the results of isothermal accelerated aging methods. These studies provide useful thermokinetics data, which are important for the safety and lifetime studies of HMX-based explosives.

Experimental

Materials and instruments

The HMX grade A with purity of 95.00 mass% (A-HMX), HMX grade B with purity of 99.50 mass% (B-HMX), and B-HMX desensitized by 5.0 mass% paraffin wax (W-HMX) were purchased from Iranian defense industries. HMX explosive quality was approved according to standard requirements and tests of HMX for use in explosive compositions, Mil-DTL-45444C [35]. Moreover, specifications of paraffin wax utilized for the preparation of W-HMX were according to Mil-W-20553 D requirements [36]. For the preparation of W-HMX, HMX particles were dispersed in hot water, at temperature of 90.0 °C, thereafter paraffin wax was added gently to solution during stirring. Finally, the temperature of materials was reduced slowly, and the product was filtered and dried. The particle size of samples was in the range of 80–150 μm .

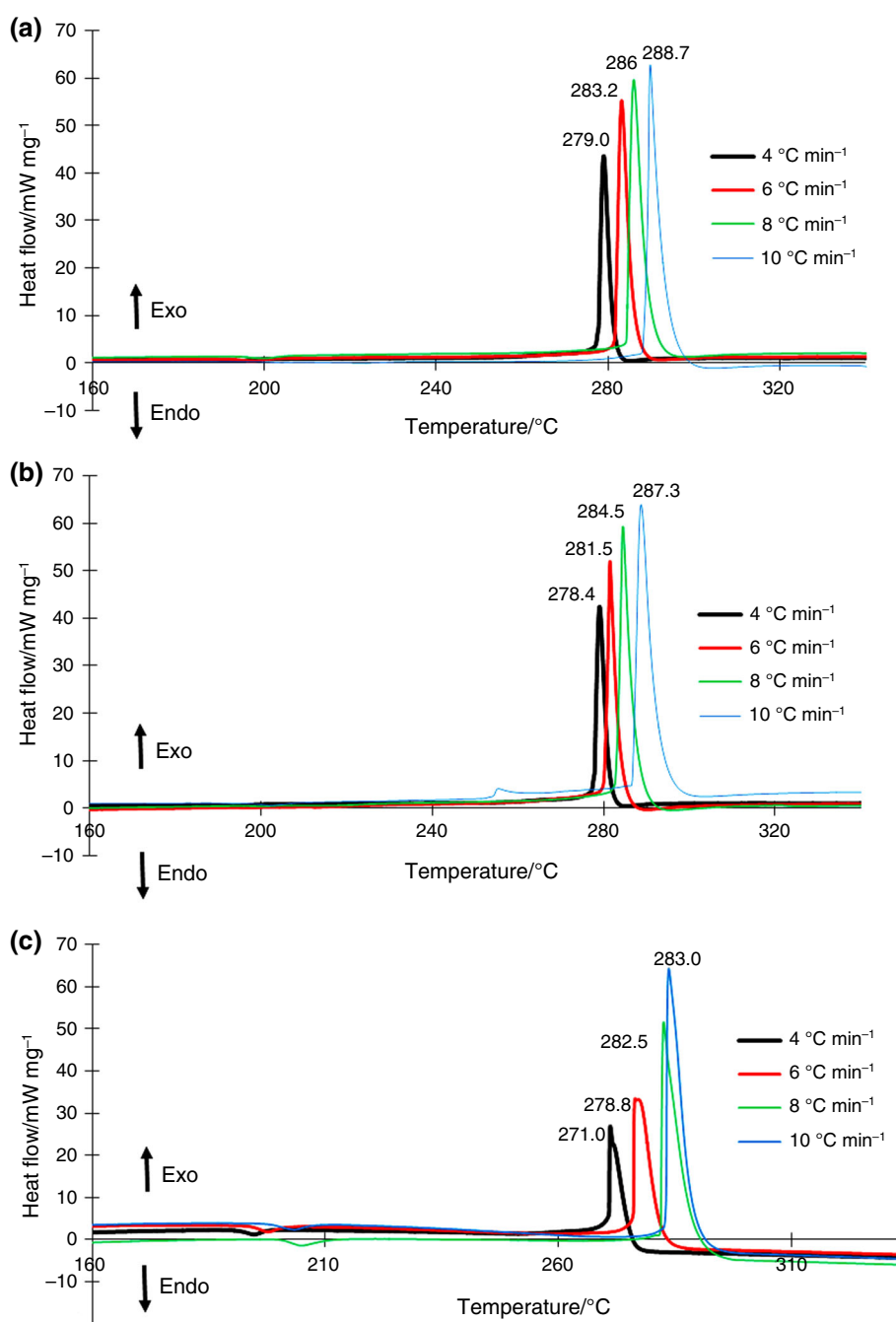
Simultaneous DSC and TG analyses measurements were performed using a PerkinElmer thermal analyzer, model STA 6000. The experiments were carried out using almost 0.53 mg of samples in an alumina pan, and at heating rates of 4, 6, 8, and 10 °C min^{-1} from 30 °C up to 350 °C, using dynamic Argon flowing atmosphere at a rate of 20 $\text{cm}^3 \text{min}^{-1}$. In addition, the isothermal accelerated aging experiments were carried out by placing almost 2.0 g of samples in an open alumina pan, at the temperature of 145.0 and 155.0 °C.

Results and discussions

DSC/TG studies

The DSC curves for A-HMX, B-HMX, and W-HMX under Argon atmosphere and the heating rates of 4, 6, 8, and 10 °C min^{-1} are illustrated in Fig. 1. To obtain reliable kinetic evaluation, there is need to exert the multiple heating rates with a wide dynamic range [37]. The profile shape has some dependency on heating rate, especially in heating rate more and less than 2.5 °C min^{-1} with some differences in profile shapes [38]. In this research we

Fig. 1 DSC curves of HMX containing **a** 0.5 mass% RDX (B-HMX), **b** 5.0 mass% RDX (A-HMX), and **c** 5.0 mass% paraffin wax (W-HMX) at the different temperature scan rates



selected sample size and heating rates in the conditions that self-heating was not observed (0.53 mg in the heating rates $<10 \text{ }^\circ\text{C min}^{-1}$). For all of the experiments, DSC sensor responses were stable; curves of program and sample temperature versus time did not show any deviation from linear state on the decomposition temperature range. We checked the effect of two other sample mass of 3.0 and 6.0 mg in the heating rate of $10.0 \text{ }^\circ\text{C min}^{-1}$ for B-HMX. The sample temperature versus time curve showed clearly effect of self-heating; in the temperature range of

decomposition, the DSC sensor response was not stable and significantly changed from linear state. Also, peak temperature showed positive deviation near to $8.0 \text{ }^\circ\text{C}$ for the sample mass of 6.0 mg . This behavior can lead to significant systematic error in the calculation of kinetic triplets.

In the DSC curves, a small endothermic peak in the range of $190\text{--}205 \text{ }^\circ\text{C}$ is due to β -HMX to δ -HMX phase transition, and also an exothermic peak in the midway of profile is related to decomposition of HMX. In the thermal

decomposition process of HMX, some gaseous products such as CH_2O , N_2O , CO , CO_2 , NO , H_2O , and N_2 can be released [13]. The peaks became wider, taller, and shifted to higher temperature, as the heating rate increased. To be sure about the obtained data and die to heat transfer effect in DSC method, the TG method is also employed and the results are shown in Fig. 2. It is observed that RDX impurity decreases the decomposition temperature of HMX explosive from 288.7 to 254.9 °C.

Kinetic aspects

In kinetic analysis, the rate of a solid-state reaction can be assumed as a function of temperature and conversion which is generally described by [39, 40]:

$$\frac{d\alpha}{dt} = k(T)f(\alpha) \quad (1)$$

where, the first part, $k(T)$ is the rate constant that is typically shown through the Arrhenius equation:

$$k(T) = A \cdot e^{-\frac{E_a}{RT}} \quad (2)$$

where E_a is activation energy (J mol^{-1}), R is the gas constant ($\text{J mol}^{-1} \text{K}^{-1}$), A is the frequency or pre-exponential (min^{-1}) factor, and T is absolute temperature in Kelvin. Furthermore, $f(\alpha)$ is the differential conversion function or reaction model [41, 42] where α is the degree of

conversion and is calculated in DSC method using the following equation:

$$\alpha = \frac{\text{AUC}_0^T}{\text{AUC}_0^\infty} \quad (3)$$

where the denominator is the entire area of decomposition curve from onset temperature to the end point of curve and the numerator is partial area from onset temperature to the required temperature of T . Under non-isothermal conditions, Eq. (1) can often be accurately described by [26, 43]:

$$\beta \frac{d\alpha}{dT} = A \exp\left(\frac{-E_a}{RT}\right) f(\alpha) \quad (4)$$

where β is heating rate in $^\circ\text{C min}^{-1}$ at constant rate, $\beta = \frac{dT}{dt}$.

From the other point of view, some integral kinetic methods are based on the following equation, which is obtained from Eq. (4) through integration [26]:

$$g(\alpha) = \frac{A}{\beta} \int_0^T \exp\left(\frac{-E_a}{RT}\right) dT \quad (5)$$

where $g(\alpha)$ is the integral form of the reaction model that leads to a large variety of methods [41, 42].

It is necessary to obtain the kinetic triplet for the prediction of thermal behavior and mathematical calculations [44]. The conversion temperature curve (α - T) helps to understand the thermal kinetic behavior during the decomposition of sample more accurately. Although there are many different reaction models, they can be categorized into three major types called accelerating, decelerating and sigmoidal curve [26]. Figure 3 illustrates the α - T curves for A-HMX, B-HMX, and W-HMX under the heating rates of 4, 6, 8, and $10^\circ\text{C min}^{-1}$, and it can be seen that the sigmoidal model was chosen as a reaction model associated with Avrami–Erofeev or Prout–Tompkins models [45, 46].

Model-free or isoconversional method for kinetic evaluations

The principle of isoconversional methods refers to the fact that the reaction rate at constant extent of conversion is only a function of temperature [26]. These methods are independent model which are called “model-free” methods, and they allow the estimation of isoconversional values of the activation energies at progressive degrees of conversion without determining any special form of reaction model [21]. Isoconversional methods have been highly recommended to determine the actual value of E_a and are divided into different methods which include the Kissinger–Akahira–Sunose (KAS) method with Eq. (6) and can be a suitable choice for this work [26, 47]:

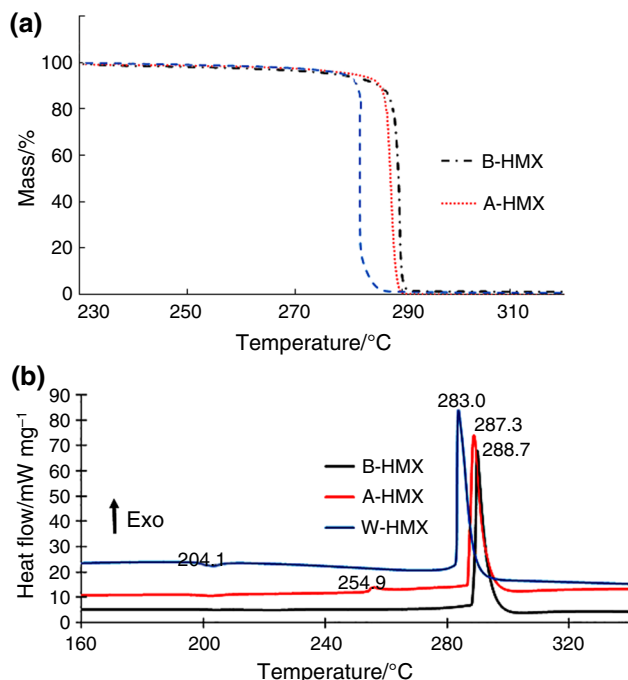


Fig. 2 a TG and b DSC curves of three samples under argon atmosphere at the heating rate of $10^\circ\text{C min}^{-1}$

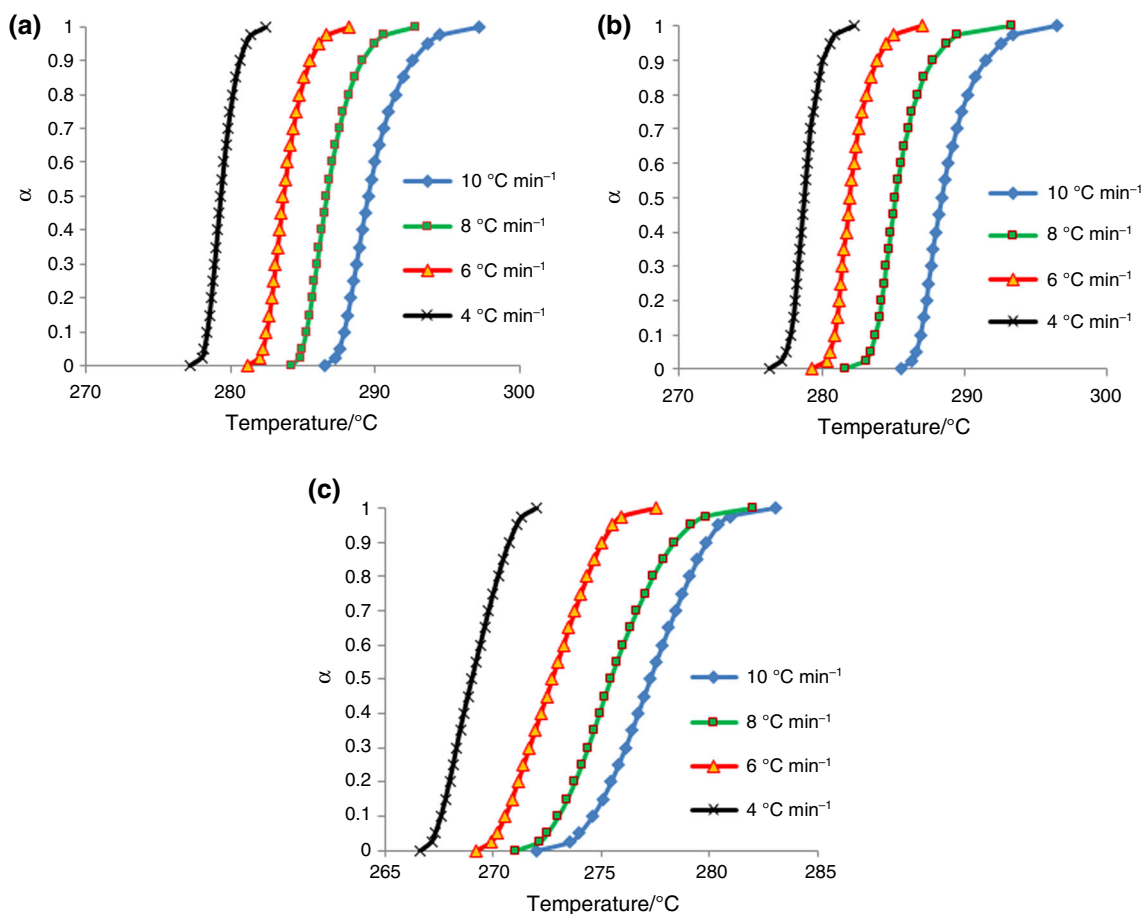


Fig. 3 Alpha-temperature (α - T) curves at different heating rates for thermal ignition of samples; **a** A-HMX, **b** B-HMX, and **c** W-HMX

$$\ln \left(\frac{\beta_i}{T_{\alpha,i}^2} \right) = \text{Const} - \frac{E_a}{RT_{\alpha,i}} \quad (6)$$

Thus, for $\alpha = \text{constant}$, the plot of $\ln(\beta_i/T_{\alpha,i}^2)$ versus $1/T_{\alpha,i}$ related to various values of α in different heating rates, is a *straight* line where the value of activation energy and pre-exponential factor can be obtained from slope and intercept, respectively [30]. In the range of 0.1–0.9 of α , the activation energies at heating rates of 4, 6, 8, 10 °C min⁻¹ were calculated. The plots obtained and activation energies from KAS equation are illustrated in Figs. 4 and 5, respectively. As shown, the activation energy of pure HMX (B-HMX) was 229.358 kJ mol⁻¹, having relatively good agreement to the results of isothermal DSC studies by Burnham with $E_a = 187.0$ – 216.0 kJ mol⁻¹ [48] and by Singh with $E_a = 197.9$ – 202.8 kJ mol⁻¹ [49]. The effect of RDX impurity and wax additive are clearly pointed on the values of activation energies which decreased to 221.053 and increased to 267.397 kJ mol⁻¹ for A-HMX and W-HMX, respectively. There is about 8.3 kJ mol⁻¹ diminution in the A grade of HMX that can be negligible or significant according to different point of views depending

on sensitivity of works. But the wax additive augments the E_a by covering the HMX molecules and desensitizing them against environmental shocks and heat of about 38.0 kJ mol⁻¹ which is considerable.

Model-fitting method by using compensation effect method

The kinetic parameters strongly depend on selection of a proper mechanism function for the process. Therefore, determination of the most probable mechanism function is highly essential. The remaining kinetic parameters of reaction model and pre-exponential factor are determined by combination of both model-free and model-fitting methods. This method has some disadvantages, and the compensation effect has been recommended as an accurate determination of reaction model and pre-exponential factor [26]. About 40 reaction models [41, 42] were exploited, and the values of E_i and A_i were extracted in each heating rate to determine a and b compensation parameters. The reaction models were tested via the differential and integral forms of equation as follows:

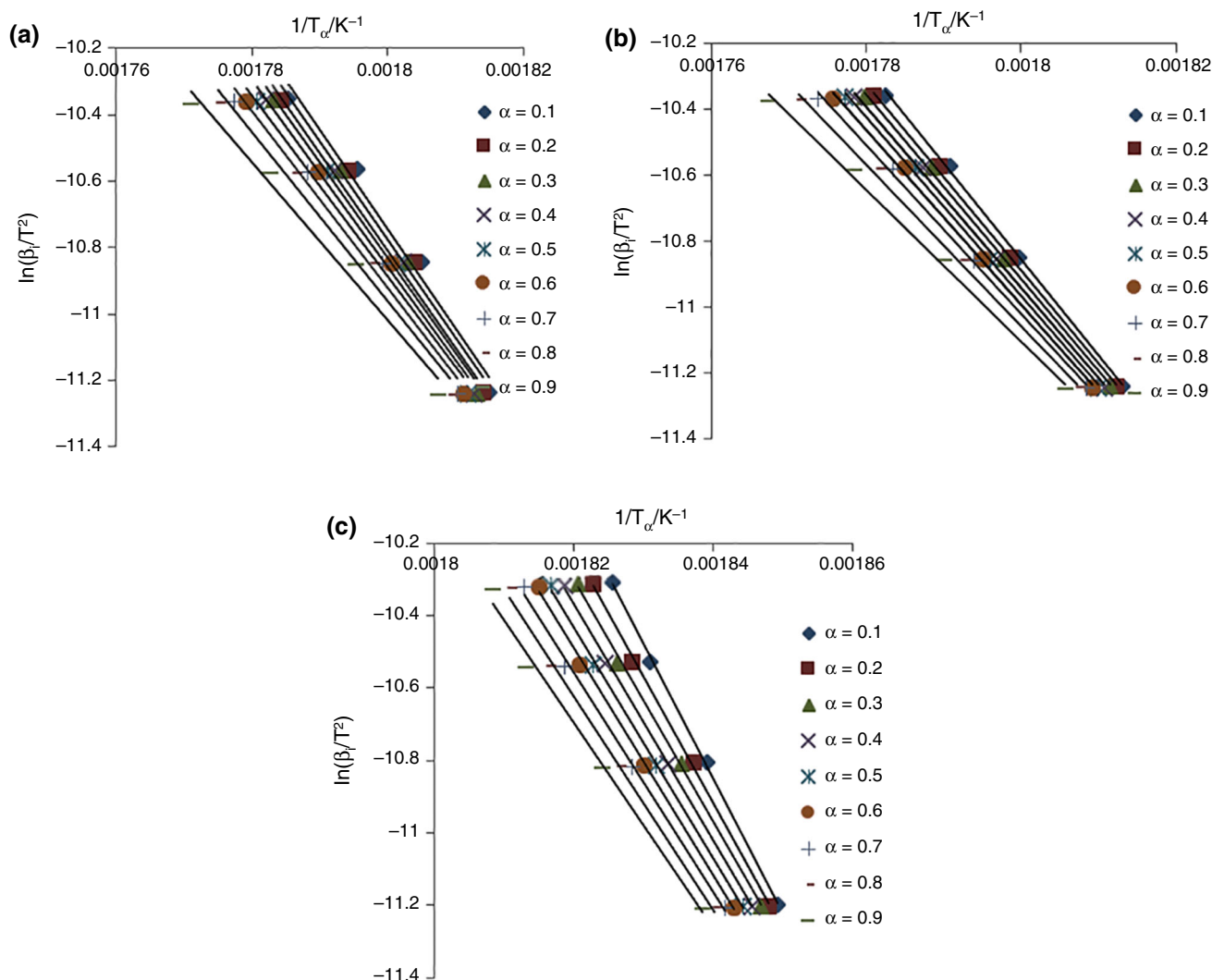


Fig. 4 KAS plots for the samples of **a** B-HMX, **b** A-HMX and **c** W-HMX at the extent of conversion between $\alpha = 0.1$ – 0.9 at four heating rates of 4, 6, 8 and $10\text{ }^{\circ}\text{C min}^{-1}$

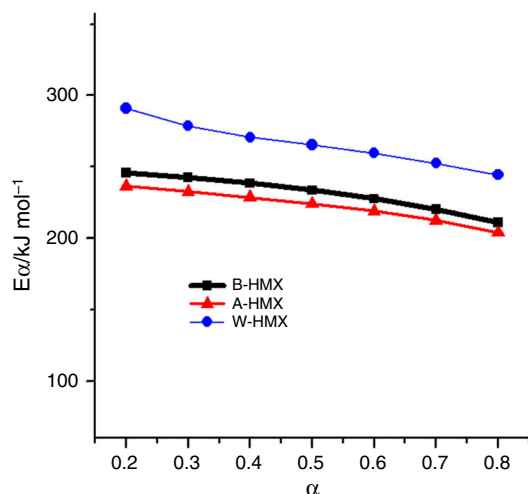


Fig. 5 Activation energies versus the extent of conversion between $\alpha = 0.2$ – 0.8 at four heating rates of 4, 6, 8, $10\text{ }^{\circ}\text{C min}^{-1}$

$$\ln \frac{\frac{d\alpha}{dT}}{f(\alpha) \frac{E_{\alpha}(T-T_0)}{RT^2+1}} = -\frac{E_{\alpha}}{RT} + \ln \left[\frac{A}{B} \right] \quad (7)$$

and

$$\ln \left[\frac{g(\alpha)}{T-T_0} \right] = -\frac{E_{\alpha}}{RT} + \ln \left[\frac{A}{B} \right] \quad (8)$$

where according to these equations, the plot of $\ln \left[\frac{(d\alpha/dT)/f(\alpha)}{[E_{\alpha}(T-T_0)/RT^2+1]} \right]$ versus $1/T$ and $\ln \left[\frac{g(\alpha)}{(T-T_0)} \right]$ versus $1/T$ at different heating rates of β_i can be obtained by linear regression. This reaction model is the most likely mechanism function, which results in the most linearity in plots with a linear regression coefficient of R^2 close to 1.0.

According to compensation method, there are several E_i and A_i at same heating rate which represents each reaction model. The obtained E_i and A_i were substituted in

following equation, and the values of a and b were determined.

$$\ln A_i = aE_i + b \quad (9)$$

Therefore, the value of A_0 can be achieved by using a , b , and E_0 , and the activation energy is obtained from model-free method, using Eq. (10):

$$\ln A_0 = aE_0 + b \quad (10)$$

The results are presented in Table 1. The experimental numerical values of $f(\alpha)$ were compared against the theoretical dependencies which were obtained from the $f(\alpha)$ equations to identify the best matching model. This was applied for all the reaction models, and finally the mechanism function of Avrami–Erofeev A2 appeared as the best pattern due to the minimum differences between experimental and theoretical data (see Fig. 6). Here, using non-linear regression method, the difference between theoretical and experimental $f(\alpha)$ was calculated through the residual sum of square. Therefore, Avrami–Erofeev A2 model can be selected as the most probable model. Moreover, the results of Table 1 clearly indicate that the paraffin wax increases the activation energy and pre-exponential factor in W-HMX, and the RDX impurity reduces these parameters in A-HMX. Here, the reaction model has not mutated because of impurity or wax additive.

Mass loss predictions and accelerated aging results

Lifetime prediction is one of the important applications of kinetic. The lifetime of a material is the time after which the material loses its properties to an extent that it cannot fulfill efficiently, the function for which it was created [26]. In this work, the 5.0% conversion or mass loss is the limiting extent of decay beyond which the sample becomes unusable. Although aging is affected by different factors, it is mostly caused by temperature. In fact, a combination of non-isothermal and isothermal experiments is the best method to properly establish kinetic and mass loss studies. The results of isothermal experiments are studied just as a better view to perceive the aging process. In isothermal method, using low temperatures in range of interest is impractical and boring and consumes a lot of time, while the upper temperature gives more accurate and faster

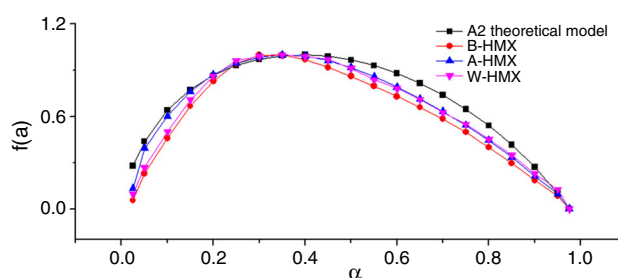


Fig. 6 Plots of theoretical and experimental $f(\alpha)$ against various conversion at heating rate of $4\text{ }^{\circ}\text{C min}^{-1}$

estimation of aging. The life time or mass loss comparison of samples is determined using the following equation:

$$t_{\alpha} = \frac{g(\alpha)}{Ae^{-E/RT_0}} \quad (11)$$

where T_0 is the constant temperature at which the samples were kept in oven. In Eq. (11), the triplet kinetic is required, and it can be determined from either isothermal or non-isothermal experiments. The isothermal experiments were conducted in two temperatures of 145.0 and $155.0\text{ }^{\circ}\text{C}$, and reaction conversion was monitored in terms of mass loss. The isothermal and theoretical prediction plots are shown in Fig. 7, and the interest data were extracted and are shown in Table 2. It is evident that there is better agreement in higher temperature between experiment and calculated graphs. Wax additive increases the lifetime while impurity reduces it. There is unfavorable agreement in case of W-HMX in low temperature due to polymeric lattice which was created using triplet wax. As an estimation, the aging in ambient temperature of $25.0\text{ }^{\circ}\text{C}$ was found around 9.22×10^{12} , 3.74×10^{11} , and 3.17×10^{15} days for B-HMX, A-HMX, and W-HMX, respectively. In non-isothermal kinetic studies, modelling of decomposition data of materials were performed in the temperature range near to $270\text{--}300\text{ }^{\circ}\text{C}$ (see Fig. 1), so expanding the predicted results to very lower temperatures, that usually are important in lifetime studies, can lead to significant experimental errors. Here, it was emphasize on the accuracy of predictions in the two selected temperatures of 145 and $155\text{ }^{\circ}\text{C}$, with only $10.0\text{ }^{\circ}\text{C}$ difference in temperature. It is clear that by increasing in the accelerated aging temperature, the accuracy of predicted mass loss values are improved.

Table 1 Kinetic triplets of three types of HMX explosive by means of model-fitting method

	$E_a/\text{kJ mol}^{-1}$ (DSC)	$E_a/\text{kJ mol}^{-1}$ (TG)	A/min^{-1}	Mechanism function
A-HMX	221.053	218.377	$3.758\text{E}+21$	$A2 [\ln(1 - \alpha)]^{1/2}$
B-HMX	229.358	224.003	$4.345\text{E}+20$	$A2 [\ln(1 - \alpha)]^{1/2}$
W-HMX	267.37	259.211	$5.77\text{E}+25$	$A2 [\ln(1 - \alpha)]^{1/2}$

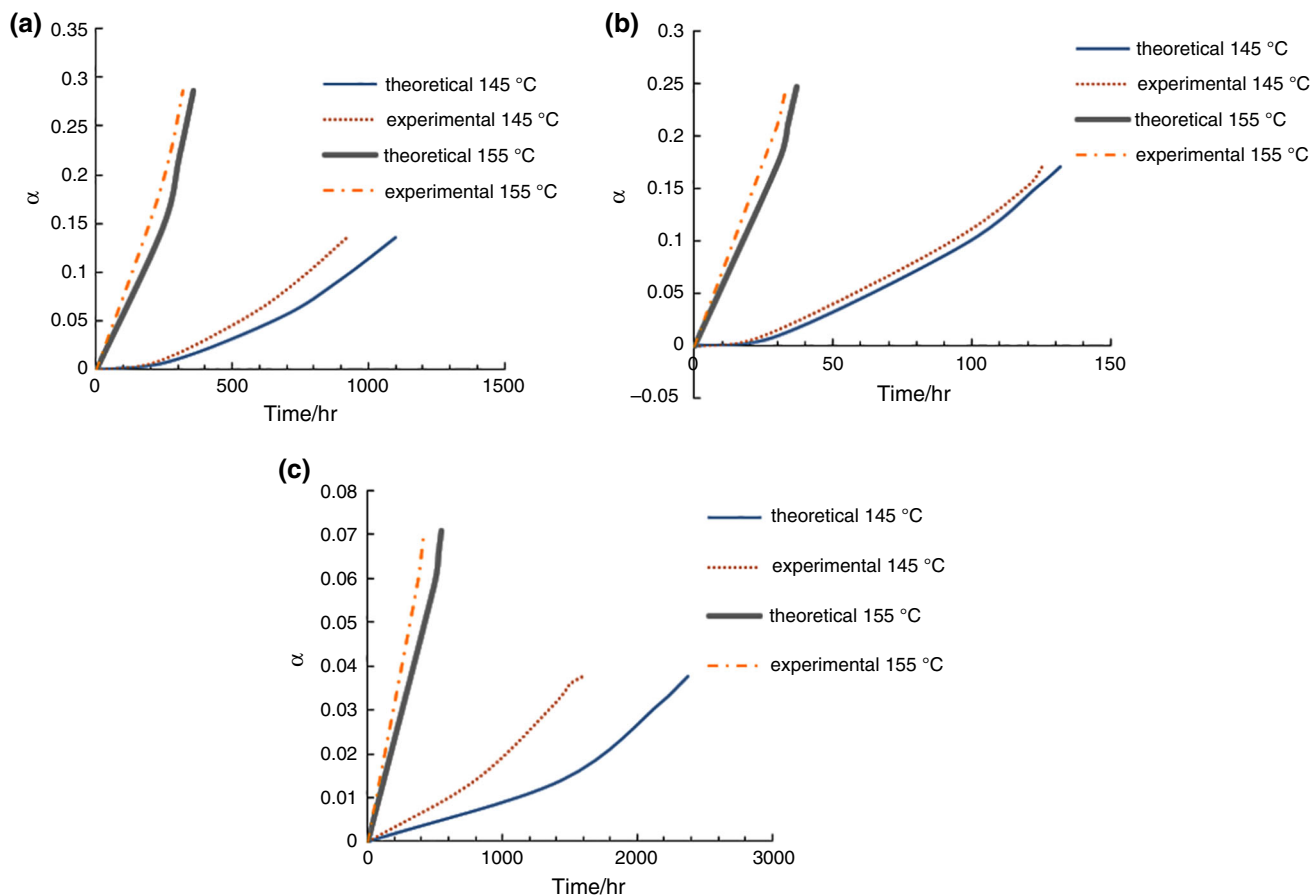


Fig. 7 Experimental and theoretical isothermal mass loss prediction versus extent of conversion plots at temperatures of 145 and 155 °C for **a** B-HMX, **b** A-HMX, and **c** W-HMX

Table 2 Thermal aging in terms of day to reach 5.0 mass% mass loss in the two isothermal temperatures

Aging temperature	B-HMX		A-HMX		W-HMX	
	Cal.	Exp.	Cal.	Exp.	Cal.	Exp.
145 °C	25.8	17.7	2.6	2.37	99.0	66.6
155 °C	3.5	2.5	0.37	0.29	17.7	13.33

Conclusions

The major aim of this experiment was to compare the effects of RDX impurity (A-HMX) and desensitizing wax (W-HMX) on the HMX thermal decomposition kinetics. The results demonstrated that thermal decomposition reaction models of HMX and the two mixtures were in line with Avrami–Erofeev A2 model. On the other hand, the decomposition temperatures and the activation energies in the various degrees of conversions were slightly decreased in the presence of RDX and were increased with the use of desensitizing paraffin wax. The accelerated aging experiments and predicted lifetime studies revealed that pure HMX and the presence of wax lead to

longer period for the decomposition of 5.0 mass% of HMX explosive. Therefore, it is highly recommended to desensitize HMX with some wax additives for more safety and longtime storage capabilities.

Acknowledgements The authors wish to thank Malek Ashtar University of technology for supporting of this work.

References

1. Fedoroff BT, Sheffield OE. Encyclopedia of explosives and related items, PATR 2700. Dover: Picatinny Arsenal; 1966.
2. Galante E, Haddad A, Marques N. Application of explosives in the oil industry. *Int J Oil Gas Coal Eng.* 2013;1(2):16–22.
3. Agrawal JP, Hodgson R. Organic chemistry of explosives. Hoboken, NJ: Wiley; 2007.
4. US Army, Detail Specification H. Military Standard MIL-DTL-45444C. US Department of Defence; 1996.
5. Van der Heijden AE, Bouma RH. Crystallization and Characterization of RDX, HMX, and CL-20. *Cryst Growth Des.* 2004;4(5):999–1007.
6. Hammer Johansen Ø, Digre Kristiansen J, Gjersøe R, Berg A, Halvorsen T, Smith KT, et al. RDX and HMX with reduced sensitivity towards shock initiation—RS-RDX and RS-HMX. *Propellant Explos Pyrotech.* 2008;33(1):20–4.

7. Shu-zhi H, Deng-Li L. Preparation and performance testing of reduced sensitivity-HMX. *Shanxi Chem Ind.* 2010;3:022.
8. Agrawal JP. High energy materials: propellants, explosives and pyrotechnics. Hoboken, NJ: Wiley; 2010.
9. Explosives M. Report TM-9-1300-214. Headquarters, Department of the Army; 1984.
10. Risse B, Schnell F, Spitzer D. Synthesis and desensitization of nano- β -HMX. *Propellant Explos Pyrotech.* 2014;39(3):397–401.
11. Y-b LI, H-j Huang, Huang H, S-b LI, L-f Guan. Desensitizing technology of high quality HMX by coating. *Chin J Energy Mater.* 2012;50:005.
12. Wu Y-Q, Huang F-L. Experimental investigations on a layer of HMX explosive crystals in response to drop-weight impact. *Combust Sci Technol.* 2013;185(2):269–92.
13. Peng D-J, Chang C-M, Chiu M. Thermal reactive hazards of HMX with contaminants. *J Hazard Mater.* 2004;114(1):1–13.
14. ASTM E. 698-05 Standard test method for arrhenius kinetic constants for thermally unstable materials using differential scanning calorimetry and the flynn. *Wall/Ozawa Method*; 2005.
15. Pouredal HR, Damiri S, Ghaemi EF. Non-isothermal studies on the thermal decomposition of C4 explosive using the TG/DTA technique. *Cent Eur J Energy Mater.* 2014;11(3):405–16.
16. Burnham AK, Weese RK, Andrzejewski WJ. Kinetics of HMX and CP decomposition and their extrapolation for lifetime assessment. In: 36th International Annual Conference & 32nd International Pyrotechnics Seminar Karlsruhe, Germany; 2005.
17. Vogelsanger B. Chemical stability, compatibility and shelf life of explosives. *Chim Int J Chem.* 2004;58(6):401–8.
18. Chiu MH, Prenner EJ. Differential scanning calorimetry: an invaluable tool for a detailed thermodynamic characterization of macromolecules and their interactions. *J Pharm Bioallied Sci.* 2011;3(1):39.
19. Yao M, Chen L, Yu J, Peng J. Thermoanalytical investigation on pyrotechnic mixtures containing Mg–Al alloy powder and barium nitrate. *Procedia Eng.* 2012;45:567–73.
20. Liao S-W, Hsieh C-C, Li K-Y, Tsai S-Y, Tseng J-M, Li J-S, et al. Storage lifetime management and thermal hazard assessment of thermally reactive material. *J Therm Anal Calorim.* 2014;116(1): 205–14.
21. Vyazovkin S, Wight CA. Model-free and model-fitting approaches to kinetic analysis of isothermal and nonisothermal data. *Thermochim Acta.* 1999;340:53–68.
22. Chen G, Lee C, Kuo Y-L, Yen Y-W. A DSC study on the kinetics of disproportionation reaction of (hfac) Cu I (COD). *Thermochim Acta.* 2007;456(2):89–93.
23. Ribeiro B, Nohara L, Oishi S, Costa M, Botelho E. Nonoxidative thermal degradation kinetic of polyamide 6, 6 reinforced with carbon nanotubes. *J Thermoplast Compos Mater.* 2013;26(10): 1317–31.
24. Han Y, Chen H, Liu N. New incremental isoconversional method for kinetic analysis of solid thermal decomposition. *J Therm Anal Calorim.* 2011;104(2):679–83.
25. Janković B, Mentus S, Janković M. A kinetic study of the thermal decomposition process of potassium metabisulfite: estimation of distributed reactivity model. *J Phys Chem Solids.* 2008;69(8): 1923–33.
26. Vyazovkin S, Burnham AK, Criado JM, Pérez-Maqueda LA, Popescu C, Sbirrazzuoli N. ICTAC Kinetics Committee recommendations for performing kinetic computations on thermal analysis data. *Thermochim Acta.* 2011;520(1):1–19.
27. Pinheiro G, Lourenco V, Iha K. Influence of the heating rate in the thermal decomposition of HMX. *J Therm Anal Calorim.* 2002;67(2):445–52.
28. Lin C-P, Chang Y-M, Tseng J-M, Shu C-M. Comparisons of nth-order kinetic algorithms and kinetic model simulation on HMX by DSC tests. *J Therm Anal Calorim.* 2010;100(2):607–14.
29. Ordzhonikidze O, Pivkina A, Frolov Y, Muravyev N, Monogarov K. Comparative study of HMX and CL-20: thermal analysis, combustion and interaction with aluminium. *J Therm Anal Calorim.* 2011;105(2):529–34.
30. Li S, Jiang Z, Yu S. Thermal decomposition of HMX influenced by nano-metal powders in high energy fuel. *Fuel Chem Div Prepr.* 2002;47(2):596.
31. Liao L-Q, Yan Q-L, Zheng Y, Song Z-W, Li J-Q, Liu P. Thermal decomposition mechanism of particulate core-shell KClO_3 -HMX composite energetic material. *Indian J Eng Mater Sci.* 2011;18(5): 393–8.
32. Tarver CM, Tran TD. Thermal decomposition models for HMX-based plastic bonded explosives. *Combust Flame.* 2004;137(1): 50–62.
33. Yan Q-L, Zeman S, Zhao F-Q, Elbeih A. Noniso-thermal analysis of C4 bonded explosives containing different cyclic nitramines. *Thermochim Acta.* 2013;556:6–12.
34. Vyazovkin S. A unified approach to kinetic processing of non isothermal data. *Int J Chem Kinet.* 1996;28(2):95–101.
35. US Army. HMX (Cyclotetramethylenetetranitramine). MIL-H-45444B, Military specification. 1992.
36. US Army. Military Specification Wax, Desensitizing. MIL-W-20553D1976.
37. Vyazovkin S, Sbirrazzuoli N. Isoconversional kinetic analysis of thermally stimulated processes in polymers. *Macromol Rapid Commun.* 2006;27(18):1515–32.
38. Makhov M. In: Proceedings of the 36th international annual conference of ICT and 32nd international pyrotechnics seminar. 2005.
39. Brown ME, Dollimore D, Galwey AK. Reactions in the solid state. Amsterdam: Elsevier; 1980.
40. Giese B, Bamford CH, Tipper CFH, et al. Comprehensive chemical kinetics, Vol. 16, liquid-phase oxidation, Elsevier, Amsterdam 1980. 264 Seiten, Preis: US \$87.75. *Ber Bunsenges Phys Chem.* 1981;85(9):721–2.
41. Starink M. The determination of activation energy from linear heating rate experiments: a comparison of the accuracy of iso-conversion methods. *Thermochim Acta.* 2003;404(1):163–76.
42. Ram IS, Singh K. Study of crystallization process in $\text{Se}_{80}\text{In}_{10}\text{Pb}_{10}$ by iso-conversional methods. *J Crys Process Technol.* 2013;3: 49–55.
43. Janković B. Kinetic analysis of the nonisothermal decomposition of potassium metabisulfite using the model-fitting and isoconversional (model-free) methods. *Chem Eng J.* 2008;139(1): 128–35.
44. Georgieva V, Zvezdova D, Vlaev L. Non-isothermal kinetics of thermal degradation of chitosan. *Chem Cent J.* 2012;6(1):1–10.
45. Akbar J, Iqbal MS, Massey S, Masih R. Kinetics and mechanism of thermal degradation of pentose-and hexose-based carbohydrate polymers. *Carbohydr Polym.* 2012;90(3):1386–93.
46. Khawam A, Flanagan DR. Solid-state kinetic models: basics and mathematical fundamentals. *J Phys Chem B.* 2006;110(35): 17315–28.
47. Akahira T, Sunose T. Method of determining activation deterioration constant of electrical insulating materials. *Res Rep Chiba Inst Technol (Sci Technol).* 1971;16:22–31.
48. Burnham AK, Weese RK. Thermal decomposition kinetics of HMX. Department of Energy: United States; 2005.
49. Singh G, Felix SP, Soni P. Studies on energetic compounds part 28: thermolysis of HMX and its plastic bonded explosives containing Estane. *Thermochim Acta.* 2003;399(1):153–65.